Human Deltoid Muscle Time-Dependent Response to Axillary Nerve Injury: Fatty Atrophy, Satellite Cell Abundance, and Motor Endplate Degeneration

Amanda Tedesco[1], Luigi Gonzales, Saman Andalib, Vivian Y Chen[2], Michael Hicks, Tyler Johnston, Oswald Steward[3], Ranjan Gupta[4]
[1]University of California Irvine School of Medicine, [2]Orthopedics Department, University of California, [3]University of California Irvine, [4]Univ of California Med Ctr

INTRODUCTION:

While it is widely known that axillary nerve injuries produce profound functional deficits and disability, there is limited understanding as to what happens to the deltoid muscle on a structural and cellular level after denervation injury in humans. Increased interest in the rotator cuff musculature has begun to elucidate complexities of how unique muscle groups respond to pathologies affecting them—including the predominance of fibrosis versus fatty infiltration, variations in fat distribution patterns, and preferential atrophy of different myofiber types based on type of injury [1-3]. However, research on the deltoid response to denervation injury remains extremely limited. As target muscle integrity, fatty infiltration, and motor endplate (MEP) preservation are important factors that influence functional outcomes following reinnervation and other treatment strategies, we present novel data characterizing how nerve injury impacts fat content, myofiber atrophy, muscle stem cell (MuSC) density, and MEP morphologic complexity in HUMAN deltoid muscle.

METHODS:

With IRB approval, healthy (n=5, age 63-79 years) and denervated (n=5, age 22-68 years) deltoid muscle biopsies were obtained from patients undergoing standard-of-care surgeries. Samples were cryosectioned and stained with Oil Red O for fat analysis, followed by immunostaining for Pax7, MF20, and laminin to identify MuSCs, myofibers, and basal lamina, respectively. MuSCs were counted and normalized to myofiber number to yield MuSC density (MuSCs/100 myofibers), and myofiber cross-sectional areas (CSA) were generated. Samples were also stained for acetylcholine receptor-α, neurofilament, and synaptophysin for 3D-characterization of MEP morphology and health. Statistical analyses comparing control and denervated sample fat content, MuSC density, and mean myofiber CSA were performed using one-way ANOVA.

RESULTS:

Fat content was found to be similar between control and denervated deltoids up to 8 months from injury but was significantly increased at 25 months and 10 years post-injury compared to healthy controls ($p<0.0001$). Interestingly, fat was localized to the perimysium with no evidence of endomysial fatty infiltration in either control or denervated deltoids. Denervated muscle MuSC density was comparable to control up to 25 months post-injury but was markedly increased at 10 years post-injury ($p<0.0001$). Mean myofiber CSA was decreased at all timepoints after injury compared to control ($p<0.0001$); however, myofiber CSA variability was greatest at 10 years post-injury. There were significantly higher proportions of degenerated MEPs (intermediate and plaque morphology) at all timepoints post-injury compared to control, with degree of degeneration correlating with time from injury.

DISCUSSION AND CONCLUSION:

Skeletal muscle denervation results in fatty degeneration and time from denervation to reconstructive surgery is known to be a critical factor affecting patient functional outcomes. While the timeline of muscle and neuromuscular junction deterioration has been studied in animal models, there is limited extrapolation to the human condition. Our study is the first to detail histologic analysis of human denervated deltoid muscle showing increasing perimysial fat content, decreasing MuSC density, reduced myofiber mean CSA, and increasing MEP degeneration with time post-denervation. Interestingly, we observed an absence of endomysial fat across all samples, and a late increase in myofiber size variability after denervation. These data helps to clarify the sequence of events of human skeletal muscle degeneration following denervation: 1) MEP degeneration, 2) myofiber atrophy, 3) perimysial fatty infiltration, and 4) increased MuSC density. Our findings pose the important question of whether MuSC or fibroadipogenic progenitor cell dysregulation is the source of skeletal muscle fatty infiltration, or whether early muscle atrophy and extracellular matrix deposition creates an environment that stimulates hypertrophy of local adipocytes as a maladaptive attempt to preserve muscle/myotendinous biomechanics. This work also calls for further investigation of the role that neural stimulation and MEP preservation—or lack thereof—plays in fatty degeneration so as to more clearly delineate the pathogenesis and mechanisms of muscle response to injury.

REFERENCES: [1] Wieser K, et al. Muscle Degeneration Induced by Sequential Release and Denervation of the Rotator Cuff Tendon in Sheep. *Orthop J Sports Med*. 2021;9(8):23259671211025302. Published 2021 Aug 16. doi:10.1177/23259671211025302.

[2] Beeler S, et al. A comparative analysis of fatty infiltration and muscle atrophy in patients with chronic rotator cuff tears and suprascapular neuropathy. *J Shoulder Elbow Surg*. 2013;22(11):1537-1546.

[3] Rowshan, K; Hadley, S; Caiozzo, VJ; Lee, TQ; Gupta, R. Development of fatty atrophy after neurologic and rotator cuff injuries in an animal model of rotator cuff pathology. *J Bone & Joint Surgery*92(13): 2270-8, 2010. PMID: 20926720.

ACKNOWLEDGEMENTS: This work was supported by NIH NIA AG081739 (RG).

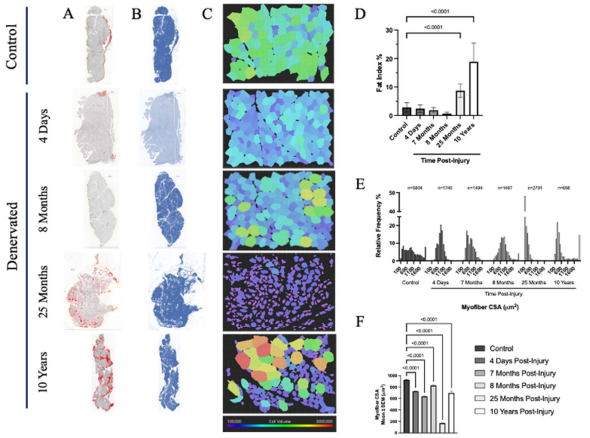

Figure 1. Representative images of Oil Red O-stained fat (A) as a proportion of total sample area (B), shown graphically as fat index percentage (D). Myofiber CSA quantification shown as representative color-scale images at 10X magnification (C), myofiber CSA relative frequency distributions (E), and mean myofiber CSA comparisons (F).

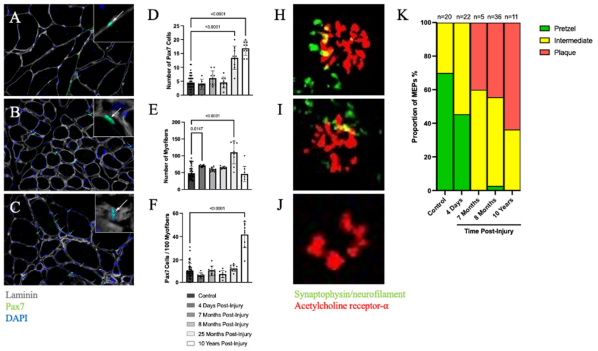

Figure 2. Representative images of control (A), 7 months post-injury (B), and 10 years post-injury (C) deltoid muscle at 20X magnification, with image insets demonstrating Pax7+ DAPI+ MuSCs. Number of Pax7 cells (D) normalized to number of myofibers (E) in an imaging field to yield Pax7 cell density (F). Classification of MEP morphology as high complexity pretzel (H), intermediate (I), or low complexity plaque (J). Quantification of MEP morphology as a proportion of total MEPs observed (K).